



Received: 30 June 2015 – Accepted: 11 August 2015 – Published: 31 August 2015

Correspondence to: J. Mohn (joachim.mohn@empa.ch)

Published by Copernicus Publications on behalf of the European Geosciences Union.

# AMTD

8, 8925–8970, 2015

## Real-time analysis of $\delta^{13}\text{C}$ - and $\delta\text{D-CH}_4$ in ambient air with laser spectroscopy

S. Eyer et al.

Title Page

Abstract

Introduction

Conclusions

References

Tables

Figures



Back

Close

Full Screen / Esc

Printer-friendly Version

Interactive Discussion



## Abstract

In situ and simultaneous measurement of the three most abundant isotopologues of methane using mid-infrared laser absorption spectroscopy is demonstrated. A field-deployable, autonomous platform is realized by coupling a compact quantum cascade laser absorption spectrometer (QCLAS) to a preconcentration unit, called TRace gas EXtractor (TRES). This unit enhances CH<sub>4</sub> mole fractions by a factor of up to 500 above ambient levels and quantitatively separates interfering trace gases such as N<sub>2</sub>O and CO<sub>2</sub>. The analytical precision of the QCLAS isotope measurement on the preconcentrated (750 ppm, parts-per-million, μmole/mole) methane is 0.1 and 0.5‰ for δ<sup>13</sup>C- and δD-CH<sub>4</sub> at 10 min averaging time.

Based on replicate measurements of compressed air during a two-week intercomparison campaign, the repeatability of the TRES-QCLAS was determined to be 0.19 and 1.9‰ for δ<sup>13</sup>C and δD-CH<sub>4</sub>, respectively. In this intercomparison campaign the new in situ technique is compared to isotope-ratio mass-spectrometry (IRMS) based on glass flask and bag sampling and real time CH<sub>4</sub> isotope analysis by two commercially available laser spectrometers. Both laser-based analyzers were limited to methane mole fraction and δ<sup>13</sup>C-CH<sub>4</sub> analysis, and only one of them, a cavity ring down spectrometer, was capable to deliver meaningful data for the isotopic composition. After correcting for scale offsets, the average difference between TRES-QCLAS data and bag/flask sampling-IRMS values are within the extended WMO compatibility goals of 0.2 and 5‰ for δ<sup>13</sup>C- and δD-CH<sub>4</sub>, respectively. Thus, the intercomparison also reveals the need for reference air samples with accurately determined isotopic composition of CH<sub>4</sub> to further improve the interlaboratory compatibility.

## 1 Introduction

Methane (CH<sub>4</sub>) is the second most important anthropogenically emitted greenhouse gas after carbon dioxide (CO<sub>2</sub>). Its mole fraction has increased from around 722 ppb

# AMTD

8, 8925–8970, 2015

## Real-time analysis of δ<sup>13</sup>C- and δD-CH<sub>4</sub> in ambient air with laser spectroscopy

S. Eyer et al.

Title Page

Abstract

Introduction

Conclusions

References

Tables

Figures



Back

Close

Full Screen / Esc

Printer-friendly Version

Interactive Discussion







level of compatibility between laboratories for future applications on both near-source studies and measurements of unpolluted air (WMO/GAW, 2013). Additionally, the need for whole air isotopologue reference gases with well calibrated CH<sub>4</sub> mole fraction and isotopic composition to improve compatibility of measurements performed in different laboratories is discussed.

## 2 Experimental

### 2.1 Preconcentration and analysis of CH<sub>4</sub> isotopologues by TREX-QCLAS

#### 2.1.1 Requirements for the preconcentration system

The main analytical challenge in the present work is the quantification of the CH<sub>3</sub>D isotopologue considering its very low natural abundance. A further constraint is given by the spectroscopic setup, as the same optical platform is used for simultaneous measurements of the <sup>12</sup>CH<sub>4</sub>, <sup>13</sup>CH<sub>4</sub> and CH<sub>3</sub>D isotopologues. This unavoidably involves compromises regarding the spectroscopic configuration, in particular the selected optical path length and the amount of trace gas needed to achieve the necessary measurement precision for both isotope ratios. Simulation of CH<sub>4</sub> absorption spectra in the target spectral regions indicated that optimal conditions are realized at a sample gas pressure in the range of 20 to 60 hPa and for mole fractions ranging from 600 up to 1000 ppm CH<sub>4</sub>. Since the CH<sub>4</sub> mole fraction in ambient air is generally in the order of 1.8 ppm, the TREX system had to be designed to selectively extract CH<sub>4</sub> from several liter of ambient air and concentrate into a gas volume of around 20 mL (e.g. equivalent to the amount of gas in the 0.5 L absorption cell of the laser spectrometer at a pressure of 40 hPa). In order to fulfill the above requirements, significant developments and innovative solutions for both TREX and QCLAS have been accomplished.

# AMTD

8, 8925–8970, 2015

## Real-time analysis of δ<sup>13</sup>C- and δD-CH<sub>4</sub> in ambient air with laser spectroscopy

S. Eyer et al.

Title Page

Abstract

Introduction

Conclusions

References

Tables

Figures

◀

▶

◀

▶

Back

Close

Full Screen / Esc

Printer-friendly Version

Interactive Discussion



## 2.1.2 TREX: design

The basic technology of the TREX (Fig. 1) is based on the “Medusa” system (Miller et al., 2008), which was later adopted for the preconcentration of N<sub>2</sub>O and its subsequent isotope analysis by QCLAS (Mohn et al., 2010, 2012, 2013, 2014; Waechter et al., 2008; Wolf et al., 2015). The main advantages over previously developed systems (Brand, 1995) are the low trapping temperatures in combination with its independence from liquid nitrogen. Preconcentration is achieved by temperature swing adsorption on a cold trap, filled with a specific adsorbent material. The trap is first cooled down to a temperature at which its dynamic adsorbing capacity for the target substance (here CH<sub>4</sub>) is sufficiently large, while the majority of the remaining bulk gases (e.g. N<sub>2</sub>, O<sub>2</sub>, Ar) pass through. During desorption, the trap is heated stepwise to separate the target substance from co-adsorbed interfering compounds. To minimize kinetic fractionation effects, it is important to adsorb and desorb the target substance quantitatively, i.e. with nearly 100 % recovery and with a high degree of reproducibility, as discussed below.

Given the low boiling point temperature of CH<sub>4</sub> (112 K) as an indication for its volatility, the original design of the preconcentration system required major revisions in terms of cooling power to enhance its CH<sub>4</sub> adsorption capacity. In addition, the layout was designed to fit in a compact and field-deployable 19” rack system. These two requirements led to a novel approach for the trap assembly.

Empirical investigations on the previous preconcentration unit (Mohn et al., 2010) with various trap models adsorbing CH<sub>4</sub> at different temperatures showed that for a complete and reliable CH<sub>4</sub> recovery, the amount of adsorbent material (HayeSep D, Sigma Aldrich, Switzerland) had to be increased by ten-fold. This resulted in 1.8 g of HayeSep D filled in a stainless steel tubing (length 90 cm, OD 4 mm, wall thickness 0.5 mm, volume 6.4 cm<sup>3</sup>) and bracketed with glass wool (BGB Analytics AG, Switzerland) and wired mesh. HayeSep D has previously been identified as an excellent high capacity adsorbent material for CH<sub>4</sub> (Eyer et al., 2014). The tubing is curled around a custom-made aluminum standoff with an optimized wall thickness of 0.5 mm. A ther-

## AMTD

8, 8925–8970, 2015

### Real-time analysis of $\delta^{13}\text{C}$ - and $\delta\text{D-CH}_4$ in ambient air with laser spectroscopy

S. Eyer et al.

Title Page

Abstract

Introduction

Conclusions

References

Tables

Figures

◀

▶

◀

▶

Back

Close

Full Screen / Esc

Printer-friendly Version

Interactive Discussion



**Real-time analysis of  $\delta^{13}\text{C}$ - and  $\delta\text{D-CH}_4$  in ambient air with laser spectroscopy**

S. Eyer et al.

Title Page

Abstract

Introduction

Conclusions

References

Tables

Figures



Back

Close

Full Screen / Esc

Printer-friendly Version

Interactive Discussion



mal conductance paste (340 HSC, Dow Corning Inc., USA) is applied at the contact region between trap and standoff to improve heat dissipation. To further increase the adsorption capacity of the trap, the trap temperature had to be decreased to 100 K, which was not achievable with the previous preconcentration unit. Therefore, we decided for a compact Stirling cryo-cooler with a cooling capacity of  $> 20\text{ W}$  at 100 K (CryoTel GT, Sunpower Inc., USA) gaining in terms of size, weight and performance. A copper plate disk (diameter 14 cm, weight 1.4 kg) was mounted on the cold-tip of the cooler, serving as a cold-plate with large heat capacity. Furthermore, we minimized the thermal cycle time of the trap for repeated adsorption/desorption processes through a design in which the trap is movable by a linear actuator (ZLD225MM, VG Scienta Ltd, UK). During cooling, the actuator pushes the aluminum standoff against the cold-plate. The contact pressure is adjusted to 100 N using a chromium-steel corrugated spring (WF-8941-SS, Durovis AG, Switzerland) placed between standoff and actuator. Contact surfaces between standoff and copper cold-plate are polished and coated with a thin layer of heat conductance paste (340 HSC, Dow Corning Inc., USA) to improve thermal contact. Before heating, the standoff is decoupled from the cold-plate. This approach is overall faster and yields lower trap temperatures compared to the previous preconcentration unit, because the cold plate and the Stirling cooler is completely undisturbed during the heating process.

For thermal isolation of the system, the core parts of the unit, i.e., the cold-tip of the Stirling cooler, the cold-plate, and the trap are housed in a custom-made vacuum chamber evacuated to  $< 10^{-4}$  mbar with a compact turbomolecular pump station (HiCube 80 Eco, Pfeiffer Vacuum GmbH, Switzerland). The TREX unit is controlled and monitored by a custom-developed LabVIEW program (National Instruments Corp., USA) with a graphical user interface. All peripherals are connected through a 16-port serial-to-ethernet connector (Etherlite 160, Digi International Inc., USA).









study. For  $\delta\text{D-CH}_4$  no significant effect could be observed; most likely, its magnitude was within the uncertainty of the system.

$\text{CH}_4$  mole fractions in both ambient air and target gas were determined based on the analysis of pre-concentrated  $\text{CH}_4$  mole fractions ( $^{12}\text{CH}_4$ ), divided by the pre-concentration factor. This factor was computed for each cycle from the gas volume in the multipass cell and the volume of pre-concentrated air. The latter is derived from the sample gas flow and the adsorption time. As the trap additionally adsorbs small amounts of  $\text{N}_2$  and  $\text{O}_2$  (up to 4 % of the pre-concentrated sample volume, depending on the trap temperature), variations in the trap temperature also need to be considered. Finally, the  $\text{CH}_4$  mole fraction measurements were linked to the WMO-X2004 calibration scale (Dlugokencky et al., 2005) through calibration of the target gas against NOAA reference standards at Empa.

## 2.2.2 Commercial laser spectrometers

During the campaign, an off-axis integrated cavity output spectrometer (OA-ICOS,  $\delta^{13}\text{C-CH}_4$  and  $\text{CH}_4$  mole fraction, MCIA-24e-EP, Los Gatos Research, USA) provided by Utrecht University (UU), and a cavity ring-down spectrometer (CRDS,  $\delta^{13}\text{C-CH}_4$ ,  $\delta^{13}\text{C-CO}_2$ ,  $\text{CH}_4$  and  $\text{CO}_2$  mole fraction, G2201-I, Picarro Inc., USA) provided by Eawag, were deployed. The OA-ICOS analyzer operated in the MIR spectral region, while the CRDS instrument comprises a NIR laser source. OA-ICOS and the CRDS isotope analyzers were calibrated twice per day using the calibration gases CG 1 and CG 2 (Table 1) for 30 min each. These standards were diluted to ambient mole fractions ( $1955.3 \pm 6.8 \text{ ppb CH}_4$ ) with high-purity synthetic air. The dependencies of  $\delta$ -values on  $\text{CH}_4$  mole fraction were linear up to a concentration of around 2500 ppb and determined to be  $-6.35$  and  $1.18 \text{ ‰ ppm}^{-1}$  for OA-ICOS and CRDS, respectively. They varied not significantly between beginning and end of the campaign and therefore a constant factor was applied. Thereafter, for both analyzers a drift and a two-point calibration correction for  $\delta^{13}\text{C-CH}_4$  was performed based on the measurements of CG 1 and CG 2.

# AMTD

8, 8925–8970, 2015

## Real-time analysis of $\delta^{13}\text{C-}$ and $\delta\text{D-CH}_4$ in ambient air with laser spectroscopy

S. Eyer et al.

Title Page

Abstract

Introduction

Conclusions

References

Tables

Figures

◀

▶

◀

▶

Back

Close

Full Screen / Esc

Printer-friendly Version

Interactive Discussion



Finally, 30 min averages of sample data were calculated, resulting in 550 measurement points for the CRDS over the two-week period of the intercomparison campaign. The repeatability of OA-ICOS and CRDS for  $\delta^{13}\text{C-CH}_4$  was assessed based on repeated analysis of the target gas (pressurized air) every six hours for 30 min.

### 2.2.3 Bag and flask sampling

In addition to the in situ optical analyzers, manual sampling in glass flasks and Tedlar bags for subsequent IRMS laboratory analysis was performed. Glass flasks were purged for 10 min with dehumidified ( $\text{Mg}(\text{ClO}_4)_2$ , Sigma-Aldrich, Switzerland) sample gas at  $2\text{ L min}^{-1}$  using a membrane pump (KNF, Netherlands) and then filled to 2000 hPa. Air samples collected in glass flasks were analyzed for  $\delta^{13}\text{C-CH}_4$ ,  $\delta\text{D-CH}_4$  and  $\text{CH}_4$  mole fraction at the Institute for Marine and Atmospheric research Utrecht (IMAU) of Utrecht University (UU) and a selection of flasks were also analyzed by the Stable Isotope Laboratory of Max-Planck-Institute (MPI) for Biogeochemistry. Parallel to the glass flask sampling and through the same sample line, 3 L Tedlar bags (SKC Ltd., USA) were filled and subsequently analyzed for  $\delta^{13}\text{C-CH}_4$  by IRMS and  $\text{CH}_4$  mole fraction by CRDS (G1301, Picarro Inc., USA) at the Greenhouse Gas Laboratory, Department of Earth Sciences (GGLES) of the Royal Holloway University of London (RHUL). In total, 81 flask and 48 bag samples were taken at different intervals, usually at least twice per day. Additionally, intensive sampling was performed on 13 June and from 20 June 12:00 to 22 June 12:00 (LT), when both flask and bag samples were filled every one to three hours.

### 2.2.4 IRMS analysis of $\delta^{13}\text{C-CH}_4$ and $\delta\text{D-CH}_4$ in flask samples at UU

Both  $\delta\text{D}$  and  $\delta^{13}\text{C}$  of  $\text{CH}_4$  were measured by continuous flow IRMS (ThermoFinnigan Delta plus XL) (Brass and Röckmann, 2010). First a 40 mL stainless steel (SS) sample loop is filled with sample or reference air at atmospheric pressure. The air is flushed by a flow of helium carrier gas (purity 99.9999%) to the preconcentration unit ( $1/8''$

## AMTD

8, 8925–8970, 2015

### Real-time analysis of $\delta^{13}\text{C-}$ and $\delta\text{D-CH}_4$ in ambient air with laser spectroscopy

S. Eyer et al.

Title Page

Abstract

Introduction

Conclusions

References

Tables

Figures

◀

▶

◀

▶

Back

Close

Full Screen / Esc

Printer-friendly Version

Interactive Discussion







cluding a 6-port rotary valve (Valco Instruments Inc.) with a 75 cm<sup>3</sup> Swagelok stainless steel sample volume and four samples, one standard gas and a vacuum line attached. The sample is expanded into the evacuated 75 cm<sup>3</sup> volume then pushed through the preparation system with a flow of helium gas. Individual sample analysis last approximately 19 min and all sample measurements were made in triplicate. Repeatability based on 10 consecutive analyses of standard air is  $\pm 0.05\%$  or better.  $\delta^{13}\text{C-CH}_4$  values of RHUL are offset corrected by  $-0.3\%$  based on intercomparison measurements with NIWA (Lowe, 2004).

### 2.3 Calibration gases and target gas

The calibration gases CG 1 and CG 2 were prepared at Empa based on gravimetric and dynamic dilution methods from pure fossil (99.9995 %, Messer, Switzerland) and biogenic CH<sub>4</sub> (> 96 %, biogas plant Volketswil, Switzerland), diluted with high-purity synthetic air. Before use, the biogenic CH<sub>4</sub> was purified from major contaminants, mainly CO<sub>2</sub> and H<sub>2</sub>O, by flushing it through an Ascarite/Mg(ClO<sub>4</sub>)<sub>2</sub> trap. The  $\delta^{13}\text{C}$  and  $\delta\text{D-CH}_4$  values of the reference gases CG 1 and CG 2, as well as of a cylinder with pressurized air used as the target gas were calibrated against the calibration scales of the Stable Isotope Laboratory of the Max-Planck-Institute (MPI) for Biogeochemistry in Jena, Germany (Sperlich et al., 2012, 2013). Results of all analytical techniques/laboratories were corrected for the offset in the target gas between assigned value determined by MPI and respective measured values.

The CH<sub>4</sub> mole fractions of CG 1 and CG 2 were analyzed with QCLAS against commercial standards for CH<sub>4</sub> mole fractions ( $1000 \pm 20$  ppmCH<sub>4</sub> in synthetic air, Messer, Switzerland), while the target gas was analyzed by WCC-Empa against the NOAA/GMD scale by CRDS (G1301, Picarro Inc., USA). Table 1 summarizes the CH<sub>4</sub> mole fractions and  $\delta$ -values of TG, CG 1 and CG 2.

## AMTD

8, 8925–8970, 2015

### Real-time analysis of $\delta^{13}\text{C-}$ and $\delta\text{D-CH}_4$ in ambient air with laser spectroscopy

S. Eyer et al.

Title Page

Abstract

Introduction

Conclusions

References

Tables

Figures

◀

▶

◀

▶

Back

Close

Full Screen / Esc

Printer-friendly Version

Interactive Discussion



## 3 Results and discussion

### 3.1 TREX-QCLAS

#### 3.1.1 QCLAS

The QCLAS precision and stability were investigated using the Allan variance technique. Therefore, individual CH<sub>4</sub> isotopologues were measured with one second integration time over a period of a few hours, as shown in Fig. 5. From the associated Allan variance plots, an optimum averaging time of approximately 600 s can be derived, corresponding to a root mean square noise of 0.1 and 0.5‰ for δ<sup>13</sup>C-CH<sub>4</sub> and δD-CH<sub>4</sub>, respectively. The one second noise performance was determined to be in the ~ 4.0 × 10<sup>-5</sup>, which corresponds to a noise equivalent absorbance per unit path length of 5.2 × 10<sup>-9</sup> cm<sup>-1</sup> when considering the 76 m optical path.

Similar to earlier work on CO<sub>2</sub> and N<sub>2</sub>O (Tuzson et al., 2008; Waechter et al., 2008), we found also in the case of methane a linear dependence of the spectroscopically retrieved isotope ratios on the mole fractions. In a series of experiments, the magnitude of this dependence was empirically determined and verified in the range of 600–1000 ppm CH<sub>4</sub>. The coefficients were 0.0145 and -0.0521‰ ppm<sup>-1</sup> for δ<sup>13</sup>C- and δD-CH<sub>4</sub>, respectively. At each calibration phase in the intercomparison campaign, these dependencies were determined repeatedly via two-point calibration and remained stable during the two-week period.

The influence of laser temperature variation on δ<sup>13</sup>C and δD-values has been determined by systematically changing the laser heat-sink temperature over ±20 mK in steps of 3 mK, and measuring the changes observed in the retrieved isotope ratios. We found a rather strong linear dependence, i.e., 0.1 and -0.2‰ mK<sup>-1</sup> for δ<sup>13</sup>C- and δD-CH<sub>4</sub>, respectively. Thus, it was crucial not only to control the laser temperature at high-precision (≈ 1 mK), but also to record the laser temperature at high resolution and to apply a drift correction caused by this effect during data post-processing.

## AMTD

8, 8925–8970, 2015

### Real-time analysis of δ<sup>13</sup>C- and δD-CH<sub>4</sub> in ambient air with laser spectroscopy

S. Eyer et al.

Title Page

Abstract

Introduction

Conclusions

References

Tables

Figures

◀

▶

◀

▶

Back

Close

Full Screen / Esc

Printer-friendly Version

Interactive Discussion





preconcentration. The HITRAN database contains the air pressure broadening coefficients only. Consequently, any deviation in the  $N_2/O_2$  ratio leads to a bias due to this effect, as the fitting model uses improper coefficients for line profile estimation.

In order to verify this hypothesis, we deliberately changed the gas matrix composition by setting its  $O_2$ -mole fraction to 21, 37 and 53 %. For each  $O_2$ -mixing ratio the  $CH_4$  mole fraction was increased stepwise from 600 to 1000 ppm and the  $\delta^{13}C$  dependence on  $CH_4$  mole fraction was accounted for. Figure 7 shows the measured dependence of  $\delta^{13}C-CH_4$  on changing  $O_2$ -mixing ratio. The gray bars indicate the ranges of the  $O_2$ -mixing ratio of sample gas after preconcentration as determined by mass spectrometry and the resulting offset in the  $\delta^{13}C$  values obtained for individual experiments. As mentioned before, the  $\delta D-CH_4$  values showed no significant dependence on  $O_2$ -mixing ratio.

This result confirms that the  $O_2$  interference is the main source of systematic bias for  $\delta^{13}C-CH_4$ , whereas fractionation effects for both,  $\delta^{13}C$ - and  $\delta D-CH_4$  values, are insignificant. The gas matrix effect could be reduced or at least maintained stable by enhancing the temperature control of the trap to constrain the  $O_2$ -mixing ratio in the gas matrix and thereby to improve the repeatability of  $\delta^{13}C$  measurements. Another solution could be to substitute the HayeSep D adsorbent material by a candidate either exhibiting a superior selectivity for  $CH_4$  over  $O_2$  or having a larger capacity for  $CH_4$ , so that the adsorption temperature can be increased. Higher adsorption temperatures would reduce the amount of  $O_2$  trapped in the system.

### 3.2 Repeatability of analytical techniques and scale differences between laboratories

Scale differences between different analytical techniques/laboratories and their repeatability were assessed based on repeated target gas measurements (Table 2). Figure 8 shows the histograms of the target gas measurements obtained with the TREX-QCLAS:  $CH_4$  mole fraction of  $2352.0 \pm 4.4$  ppb,  $\delta^{13}C-CH_4 = -47.99 \pm 0.19$ ‰ and  $\delta D-$

## Real-time analysis of $\delta^{13}C$ - and $\delta D-CH_4$ in ambient air with laser spectroscopy

S. Eyer et al.

Title Page

Abstract

Introduction

Conclusions

References

Tables

Figures



Back

Close

Full Screen / Esc

Printer-friendly Version

Interactive Discussion



**Real-time analysis of  $\delta^{13}\text{C}$ - and  $\delta\text{D-CH}_4$  in ambient air with laser spectroscopy**

S. Eyer et al.

Title Page

Abstract

Introduction

Conclusions

References

Tables

Figures

◀

▶

◀

▶

Back

Close

Full Screen / Esc

Printer-friendly Version

Interactive Discussion



$\text{CH}_4 = -120.9 \pm 1.9\text{‰}$ . The repeatability of TREX-QCLAS was comparable to manual sampling with subsequent IRMS analysis for  $\delta\text{D-CH}_4$ , but about a factor three worse for  $\delta^{13}\text{C-CH}_4$ . The CRDS exhibited a comparable repeatability (0.24‰) to TREX-QCLAS for  $\delta^{13}\text{C-CH}_4$ , while with 0.78‰ the performance of OA-ICOS was significantly worse.

In summary, the repeatability of TREX-QCLAS, CRDS and all IRMS laboratories offer the capability to reach the extended WMO/GAW compatibility goals for  $\delta^{13}\text{C}$  and  $\delta\text{D-CH}_4$ , of 0.2 and 5‰, defined for regional scale studies (WMO/GAW, 2013), while the goals for background measuring stations of 0.02 and 1‰ for  $\delta^{13}\text{C}$  and  $\delta\text{D-CH}_4$  are beyond the performance of any of the applied techniques. A more detailed discussion is given in Sect. 3.4.

For assessing the compatibility between the instruments, IRMS measurements of MPI were chosen as the reference point, as MPI recently established a direct link to the international isotope standard scales. The data obtained from the laser spectroscopic techniques (TREX-QCLAS, CRDS and OA-ICOS) are referenced to the standards CG 1 and CG 2, analyzed by MPI, while the IRMS measurements of UU and RHUL are referenced to their respective laboratory standards. The agreement for  $\delta^{13}\text{C-CH}_4$  is within 0.1‰ for all techniques/laboratories, except the IRMS measurements of RHUL, which were 0.25‰ higher and the OA-ICOS results, which were offset by as much as  $-8.87\text{‰}$ . For  $\delta\text{D-CH}_4$ , no significant differences were observed between TREX-QCLAS and the MPI IRMS, while the UU IRMS values were 2.3‰ higher.

The ambient air measurements during the campaign were offset-corrected for differences in  $\delta^{13}\text{C}$  and  $\delta\text{D-CH}_4$  measurements of TG by individual techniques/laboratories and MPI summarized in Table 2. Differences for IRMS laboratories include differences in scales and instrumental issues, while the laser spectroscopic techniques are all calibrated using CG 1 and CG 2. The OA-ICOS data are not considered further due to the limited performance with respect to repeatability and scale offset.

### 3.3 Real-time analysis of CH<sub>4</sub> isotopic composition in ambient air

The CH<sub>4</sub> mole fraction and isotopic composition measurements in ambient air between 6 and 22 June 2014 of the various laser spectroscopic and mass spectrometric analytical techniques is shown in Fig. 9. Data of all laboratories have been offset corrected as discussed in the previous section. During the campaign, more than 250 air samples (199 samples of ambient air, 62 target gas samples) were analyzed in stand-alone operation by TREX-QCLAS and more than 120 manually taken samples were analyzed by IRMS. The CRDS data were averaged for 30 min, resulting in 550 mean values.

The CH<sub>4</sub> mole fractions exhibit a regular diurnal variation with night-time values increasing up to 2300 ppb, which is around 400 ppb higher than at daytime. When comparing the measurement data from the local weather station in Dübendorf with the measured CH<sub>4</sub>-mole fractions, the nights with the highest emissions also exhibit very low wind speed (0–7 ms<sup>-1</sup>) and, thus, leading to more stable boundary conditions. Stable boundary conditions reduce the mixing volume of emissions, which leads to a stronger CH<sub>4</sub>-signal. Variations in the  $\delta^{13}\text{C}$ - and  $\delta\text{D-CH}_4$  values display a clear anti-correlation with the mole fraction changes indicating emissions of CH<sub>4</sub> depleted in <sup>13</sup>CH<sub>4</sub> and CH<sub>3</sub>D. The compatibility of different techniques for CH<sub>4</sub> isotopic analysis in ambient air is discussed based on correlation diagrams in the next section.

### 3.4 Compatibility of analytical techniques for $\delta^{13}\text{C}$ - and $\delta\text{D-CH}_4$ in ambient air

The compatibility of different analytical techniques for CH<sub>4</sub> isotope measurements was assessed on the ambient air measurements shown in Fig. 9. Measurements were done either on identical gas samples, i.e. for IRMS measurements of glass flask samples by UU and MPI, or on simultaneously collected ambient air samples, i.e. for all other techniques (laser spectrometers and bag samples/IRMS). The  $\delta^{13}\text{C}$ - and  $\delta\text{D-CH}_4$  measurements on glass flasks by IRMS at UU were chosen as reference for this comparison, due to the much higher number of samples ( $n = 67$ ) analyzed as compared to MPI ( $n = 15$ ). Isotope data of all techniques were offset-corrected as described in Sect. 3.1

## AMTD

8, 8925–8970, 2015

### Real-time analysis of $\delta^{13}\text{C}$ - and $\delta\text{D-CH}_4$ in ambient air with laser spectroscopy

S. Eyer et al.

Title Page

Abstract

Introduction

Conclusions

References

Tables

Figures



Back

Close

Full Screen / Esc

Printer-friendly Version

Interactive Discussion







tration unit can be applied for the analysis of mole fraction and isotopic composition of other trace gases, e.g. N<sub>2</sub>O and VOCs. The potential of this technique for N<sub>2</sub>O isotopes was recently demonstrated in an extended field campaign (Wolf et al., 2015).

#### 4 Conclusion and outlook

This study presents the development and validation of a novel measurement technique, called TREX-QCLAS, for real-time analysis of the three main CH<sub>4</sub> isotopologues <sup>12</sup>CH<sub>4</sub>, <sup>13</sup>CH<sub>4</sub> and <sup>12</sup>CH<sub>3</sub>D in ambient air. The fully automated instrument is based on cryogen-free CH<sub>4</sub> preconcentration, followed by selective and high-precision isotope analysis with mid-IR QCL absorption spectroscopy.

This is the first demonstration of analyzing δ<sup>13</sup>C and δD-CH<sub>4</sub> simultaneously with one instrument in ambient air, real-time and under field conditions. The TREX-QCLAS technique was deployed in an interlaboratory comparison campaign for a period of two weeks. Data of the TREX-QCLAS instrument was compared to commercial laser spectroscopic techniques (CRDS, OA-ICOS) as well as to the established IRMS technique using flask or bag sampling. During this period, the TREX-QCLAS performed more than 250 measurement cycles, while 120 air samples were manually collected for subsequent IRMS analysis. The repeatability of TREX-QCLAS based on target gas measurements was found to be 0.19‰ for δ<sup>13</sup>C-CH<sub>4</sub> and 1.9‰ for δD-CH<sub>4</sub>, which is similar or slightly worse than the state of the art IRMS techniques. Selected noon-to-noon periods of the recorded time-series were analyzed using Keeling plots. During these intervals, the TREX-QCLAS method was able to successfully distinguish between CH<sub>4</sub> emissions with predominately microbial origin and a case with significant influences from a fossil source.

The intercomparison campaign also exposed calibration scale issues and underlined the need for CH<sub>4</sub> isotope standard gases at ambient mole fractions to improve the compatibility among different analytical techniques and laboratories. With its compactness and ability to analyze simultaneously δ<sup>13</sup>C-CH<sub>4</sub> and δD-CH<sub>4</sub> in a stand-alone opera-

### Real-time analysis of δ<sup>13</sup>C- and δD-CH<sub>4</sub> in ambient air with laser spectroscopy

S. Eyer et al.

Title Page

Abstract

Introduction

Conclusions

References

Tables

Figures



Back

Close

Full Screen / Esc

Printer-friendly Version

Interactive Discussion







## Real-time analysis of $\delta^{13}\text{C}$ - and $\delta\text{D-CH}_4$ in ambient air with laser spectroscopy

S. Eyer et al.

[Title Page](#)
[Abstract](#)
[Introduction](#)
[Conclusions](#)
[References](#)
[Tables](#)
[Figures](#)




[Back](#)
[Close](#)
[Full Screen / Esc](#)
[Printer-friendly Version](#)
[Interactive Discussion](#)


- Fischer, H., Behrens, M., Bock, M., Richter, U., Schmitt, J., Loulergue, L., Chappellaz, J., Spahni, R., Blunier, T., Leuenberger, M., and Stocker, T. F.: Changing boreal methane sources and constant biomass burning during the last termination, *Nature*, 452, 864–867, doi:10.1038/nature06825, 2008.
- 5 Fisher, R., Lowry, D., Wilkin, O., Sriskantharajah, S., and Nisbet, E. G.: High-precision, automated stable isotope analysis of atmospheric methane and carbon dioxide using continuous-flow isotope-ratio mass spectrometry, *Rapid Commun. Mass Sp.*, 20, 200–208, doi:10.1002/rcm.2300, 2006.
- IPCC: Climate Change 2013: the Physical Science Basis. Contribution of Working Group I to the Fifth Assessment Report of the Intergovernmental Panel on Climate Change, edited by: Stocker, T. F., Qin, D., Plattner, G.-K., Tignor, M., Allen, S. K., Boschung, J., Nauels, A., Xia, Y., Bex, V., and Midgley, P. M., Cambridge University Press, Cambridge, United Kingdom and New York, NY, USA, 1535 pp., doi:10.1017/CBO9781107415324, 2013.
- 10 Keeling, C. D.: The concentration and isotopic abundances of atmospheric carbon dioxide in rural areas, *Geochim. Cosmochim. Ac.*, 13, 322–334, doi:10.1016/0016-7037(58)90033-4, 1958.
- Keeling, C. D.: The concentration and isotopic abundances of carbon dioxide in rural and marine air, *Geochim. Cosmochim. Ac.*, 24, 277–298, doi:10.1016/0016-7037(61)90023-0, 1961.
- Köster, J. R., Well, R., Tuzson, B., Bol, R., Dittert, K., Giesemann, A., Emmenegger, L., Manninen, A., Cárdenas, L., and Mohn, J.: Novel laser spectroscopic technique for continuous analysis of  $\text{N}_2\text{O}$  isotopomers – application and intercomparison with isotope ratio mass spectrometry, *Rapid Commun. Mass Sp.*, 27, 216–222, doi:10.1002/rcm.6434, 2013.
- 20 Lowe, D. C.: Seasonal cycles of mixing ratio and  $^{13}\text{C}$  in atmospheric methane at Suva, Fiji, *J. Geophys. Res.*, 109, D23308, doi:10.1029/2004JD005166, 2004.
- 25 Manning, A. C., Nisbet, E. G., Keeling, R. F., and Liss, P. S.: Greenhouse gases in the Earth system: setting the agenda to 2030, *Philos. T. Roy. Soc. A.*, 369, 1885–1890, doi:10.1098/rsta.2011.0076, 2011.
- McManus, J. B., Zahniser, M. S., Nelson, D. D., Shorter, J. H., Herndon, S., Wood, E., and Wehr, R.: Application of quantum cascade lasers to high-precision atmospheric trace gas measurements, *Opt. Eng.*, 49, 111124, 1–11, doi:10.1117/1.3498782, 2010.
- 30 McManus, J. B., Zahniser, M. S., and Nelson, D. D.: Dual quantum cascade laser trace gas instrument with astigmatic Herriott cell at high pass number, *Appl. Optics*, 50, A74–A85, doi:10.1364/AO.50.000A74, 2011.

**Real-time analysis of  $\delta^{13}\text{C}$ - and  $\delta\text{D-CH}_4$  in ambient air with laser spectroscopy**

S. Eyer et al.

Title Page

Abstract

Introduction

Conclusions

References

Tables

Figures



Back

Close

Full Screen / Esc

Printer-friendly Version

Interactive Discussion



Miller, B. R., Weiss, R. F., Salameh, P. K., Tanhua, T., Grealley, B. R., Mühle, J., and Simmonds, P. G.: Medusa: a sample preconcentration and GC/MS detector system for in situ measurements of atmospheric trace halocarbons, hydrocarbons, and sulfur compounds, *Anal. Chem.*, 80, 1536–1545, doi:10.1021/ac702084k, 2008.

5 Mohn, J., Guggenheim, C., Tuzson, B., Vollmer, M. K., Toyoda, S., Yoshida, N., and Emmenegger, L.: A liquid nitrogen-free preconcentration unit for measurements of ambient  $\text{N}_2\text{O}$  isotopomers by QCLAS, *Atmos. Meas. Tech.*, 3, 609–618, doi:10.5194/amt-3-609-2010, 2010.

Mohn, J., Tuzson, B., Manninen, A., Yoshida, N., Toyoda, S., Brand, W. A., and Emmenegger, L.: Site selective real-time measurements of atmospheric  $\text{N}_2\text{O}$  isotopomers by laser spectroscopy, *Atmos. Meas. Tech.*, 5, 1601–1609, doi:10.5194/amt-5-1601-2012, 2012.

10 Mohn, J., Steinlin, C., Merbold, L., Emmenegger, L., and Hagedorn, F.:  $\text{N}_2\text{O}$  emissions and source processes in snow-covered soils in the Swiss Alps, *Isot. Environ. Health. S.*, 49, 520–531, doi:10.1080/10256016.2013.826212, 2013.

15 Mohn, J., Wolf, B., Toyoda, S., Lin, C.-T., Liang, M.-C., Brüggemann, N., Wissel, H., Steiker, A. E., Dyckmans, J., Szwece, L., Ostrom, N. E., Casciotti, K. L., Forbes, M., Gieseemann, A., Well, R., Doucett, R. R., Yarnes, C. T., Ridley, A. R., Kaiser, J., and Yoshida, N.: Interlaboratory assessment of nitrous oxide isotopomer analysis by isotope ratio mass spectrometry and laser spectroscopy: current status and perspectives, *Rapid Commun. Mass Sp.*, 28, 1995–2007, doi:10.1002/rcm.6982, 2014.

20 Monteil, G., Houweling, S., Dlugokenky, E. J., Maenhout, G., Vaughn, B. H., White, J. W. C., and Rockmann, T.: Interpreting methane variations in the past two decades using measurements of  $\text{CH}_4$  mixing ratio and isotopic composition, *Atmos. Chem. Phys.*, 11, 9141–9153, doi:10.5194/acp-11-9141-2011, 2011.

Nisbet, E. G., Dlugokenky, E. J., and Bousquet, P.: Methane on the rise-again, *Science*, 343, 493–495, doi:10.1126/science.1247828, 2014.

25 Rigby, M., Manning, A. J., and Prinn, R. G.: The value of high-frequency, high-precision methane isotopologue measurements for source and sink estimation, *J. Geophys. Res.-Atmos.*, 117, D12312, doi:10.1029/2011JD017384, 2012.

30 Santoni, G. W., Lee, B. H., Goodrich, J. P., Varner, R. K., Crill, P. M., McManus, J. B., Nelson, D. D., Zahniser, M. S., and Wofsy, S. C.: Mass fluxes and isofluxes of methane ( $\text{CH}_4$ ) at a New Hampshire fen measured by a continuous wave quantum cascade laser spectrometer, *J. Geophys. Res.-Atmos.*, 117, D10301, doi:10.1029/2011JD016960, 2012.



## Real-time analysis of $\delta^{13}\text{C}$ - and $\delta\text{D-CH}_4$ in ambient air with laser spectroscopy

S. Eyer et al.

Title Page

Abstract

Introduction

Conclusions

References

Tables

Figures

◀

▶

◀

▶

Back

Close

Full Screen / Esc

Printer-friendly Version

Interactive Discussion



- Tuzson, B., Hiller, R. V., Zeyer, K., Eugster, W., Neftel, A., Ammann, C., and Emmenegger, L.: Field intercomparison of two optical analyzers for  $\text{CH}_4$  eddy covariance flux measurements, *Atmos. Meas. Tech.*, 3, 1519–1531, doi:10.5194/amt-3-1519-2010, 2010.
- Urey, H. C.: Oxygen isotopes in nature and in the laboratory, *Science*, 108, 489–496, doi:10.1126/science.108.2810.489, 1948.
- Waechter, H., Mohn, J., Tuzson, B., Emmenegger, L., and Sigrist, M. W.: Determination of  $\text{N}_2\text{O}$  isotopomers with quantum cascade laser based absorption spectroscopy, *Opt. Express*, 16, 9239–9244, doi:10.1364/OE.16.009239, 2008.
- Werle, P.: Accuracy and precision of laser spectrometers for trace gas sensing in the presence of optical fringes and atmospheric turbulence, *Appl. Phys. B*, 102, 313–329, doi:10.1007/s00340-010-4165-9, 2010.
- Werner, R. and Brand, W.: Referencing strategies and techniques in stable isotope ratio analysis., *Rapid Commun. Mass Sp.*, 15, 501–519, doi:10.1002/rcm.258, 2001.
- WMO/GAW: GAW Report No. 213 17th WMO/IAEA Meeting on Carbon Dioxide, Other Greenhouse Gases and Related Tracers Measurement Techniques (GGMT-2013), Beijing, available at: <http://www.wmo.int/pages/prog/arep/gaw/gaw-reports.html>, 2014.
- WMO/GAW: WMO Greenhouse Gas Bulletin, available at: [http://www.wmo.int/pages/prog/arep/gaw/ghg/documents/GHG\\_Bulletin\\_10\\_Nov2014\\_EN.pdf](http://www.wmo.int/pages/prog/arep/gaw/ghg/documents/GHG_Bulletin_10_Nov2014_EN.pdf), 2014.
- Wolf, B., Merbold, L., Decock, C., Tuzson, B., Harris, E., Six, J., Emmenegger, L., and Mohn, J.: First on-line isotopic characterization of  $\text{N}_2\text{O}$  above intensively managed grassland, *Biogeosciences*, 12, 2517–2531, doi:10.5194/bg-12-2517-2015, 2015.

## Real-time analysis of $\delta^{13}\text{C}$ - and $\delta\text{D-CH}_4$ in ambient air with laser spectroscopy

S. Eyer et al.

**Table 1.** List of  $\text{CH}_4$  mole fractions and isotopic composition ( $\delta^{13}\text{C}$  and  $\delta\text{D-CH}_4$ ) of laboratory standards used in the intercomparison campaign. The indicated uncertainty is the  $1\sigma$  standard deviation for repeated analysis of the respective measurement system.

	composition	$\text{CH}_4$ [ppm]	$\delta^{13}\text{C-CH}_4^c$ [‰]	$\delta\text{D-CH}_4^c$ [‰]
CG 1	fossil/biogenic $\text{CH}_4$ in synthetic air	$938.8 \pm 3.5^a$	$-46.60 \pm 0.10$	$-250.46 \pm 1.05$
CG 2	fossil $\text{CH}_4$ in synthetic air	$1103.8 \pm 3.5^a$	$-36.13 \pm 0.10$	$-180.58 \pm 1.05$
TG	pressurized ambient air	$2.3523 \pm 0.0002^b$	$-48.07 \pm 0.10$	$-120.00 \pm 1.05$

$\text{CH}_4$  mole fractions were measured by CRDS<sup>a</sup> after dilution by a factor of 1 : 500 or<sup>b</sup> by direct measurement.

<sup>c</sup> Isotopic values were analyzed by IRMS at MPI.

Title Page

Abstract

Introduction

Conclusions

References

Tables

Figures

◀

▶

◀

▶

Back

Close

Full Screen / Esc

Printer-friendly Version

Interactive Discussion



## Real-time analysis of $\delta^{13}\text{C}$ - and $\delta\text{D}$ - $\text{CH}_4$ in ambient air with laser spectroscopy

S. Eyer et al.

Title Page

Abstract

Introduction

Conclusions

References

Tables

Figures

◀

▶

◀

▶

Back

Close

Full Screen / Esc

Printer-friendly Version

Interactive Discussion



**Table 2.** List of measured  $\delta^{13}\text{C}$ - $\text{CH}_4$  and  $\delta\text{D}$ - $\text{CH}_4$  values of the target gas (pressurized air) as reported by different analytical techniques/laboratories. The indicated uncertainty is the  $1\sigma$  standard deviation. Results of laser spectroscopic techniques are referenced to standards CG 1 and CG 2, while IRMS results were referenced to their respective laboratory standards.

	number of measurements	$\delta^{13}\text{C}$ - $\text{CH}_4$ [‰]	$\delta\text{D}$ - $\text{CH}_4$ [‰]
Glass-flask/IRMS (MPI)	1	$-48.07 \pm 0.10$	$-120.0 \pm 1.05$
TREX-QCLAS (Empa)	62	$-47.99 \pm 0.19$	$-120.9 \pm 1.9$
Glass-flask/IRMS (UU)	4	$-47.96 \pm 0.08$	$-117.7 \pm 2.0$
CRDS (Eawag)	64	$-48.04 \pm 0.24$	n.a.
OA-ICOS (UU)	10	$-56.94 \pm 0.78$	n.a.
Bag/IRMS (RHUL)	3	$-47.82 \pm 0.05$	n.a.

n.a.: not analyzed.



## Real-time analysis of $\delta^{13}\text{C}$ - and $\delta\text{D-CH}_4$ in ambient air with laser spectroscopy

S. Eyer et al.

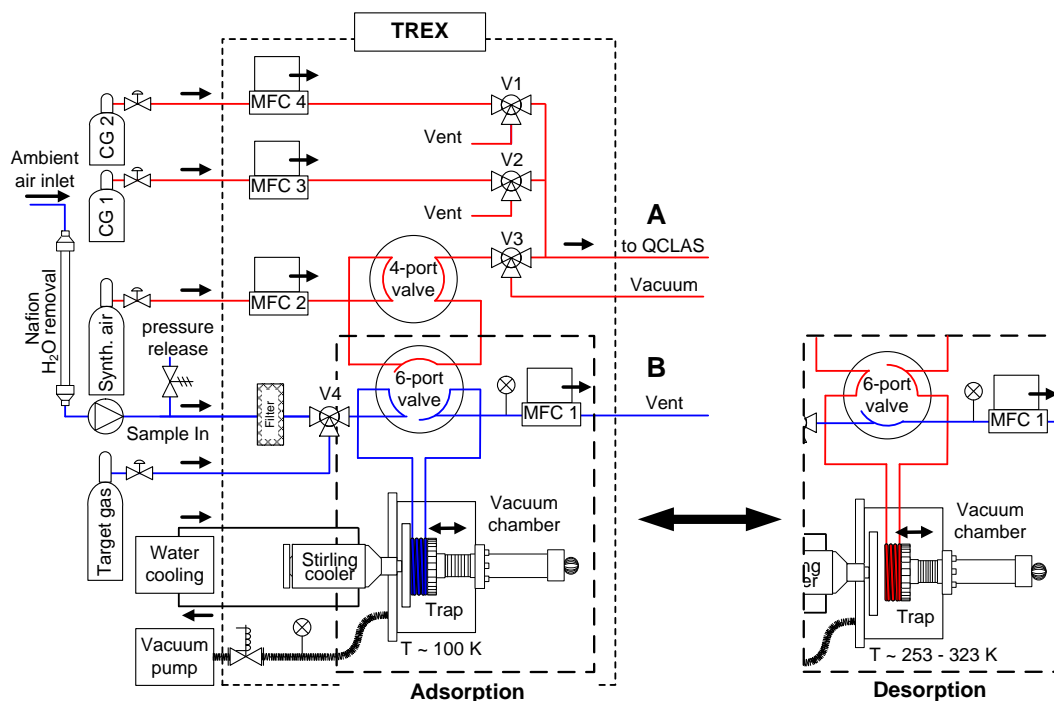


**Figure 1.** Schematics of the preconcentration unit (TREX). The blue lines indicate the flow of sample air and TG, i.e. ambient air  $\text{CH}_4$ -mole fractions, while red lines represent the flow of calibration gases and desorbed air, i.e. high  $\text{CH}_4$ -mole fraction. MFC 1-4 and V1-4 stand for mass flow controllers and 2-position valves, respectively.

Title Page

Abstract

Introduction

Conclusions

References

Tables

Figures

◀

▶

◀

▶

Back

Close

Full Screen / Esc

Printer-friendly Version

Interactive Discussion

## Real-time analysis of $\delta^{13}\text{C}$ - and $\delta\text{D}$ - $\text{CH}_4$ in ambient air with laser spectroscopy

S. Eyer et al.

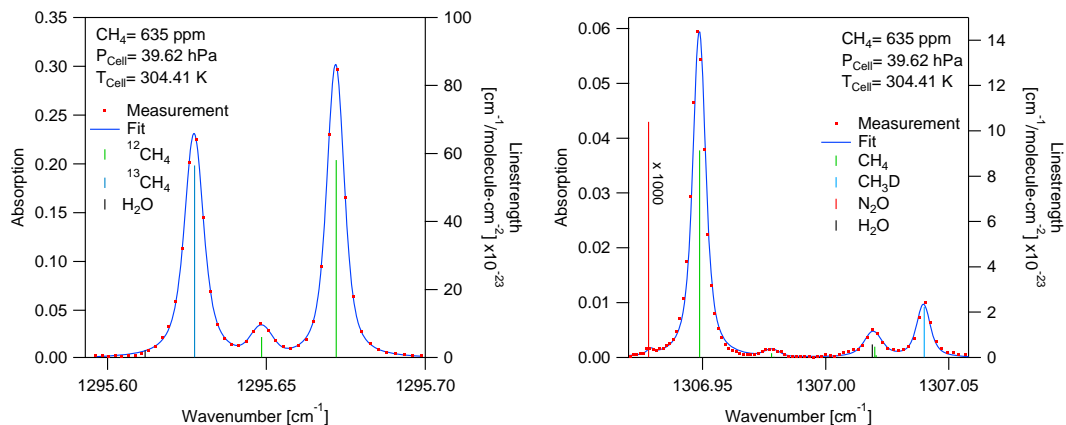


**Figure 2.** Measured absorption spectra for the determination of  $\delta^{13}\text{C}$ - (left) and  $\delta\text{D}$ - $\text{CH}_4$  (right) along with the spectral fit using Voigt-profiles and the corresponding line-strengths from the HITRAN database. Potential interferences are expected mainly from  $\text{N}_2\text{O}$  and  $\text{H}_2\text{O}$ . The spectral line of  $\text{N}_2\text{O}$  is divided by a factor of 1000 to fit in the graph, evidencing that even  $\text{N}_2\text{O}$ -mole fraction of around 300 ppb can cause severe interference.

Title Page

Abstract

Introduction

Conclusions

References

Tables

Figures

◀

▶

◀

▶

Back

Close

Full Screen / Esc

Printer-friendly Version

Interactive Discussion



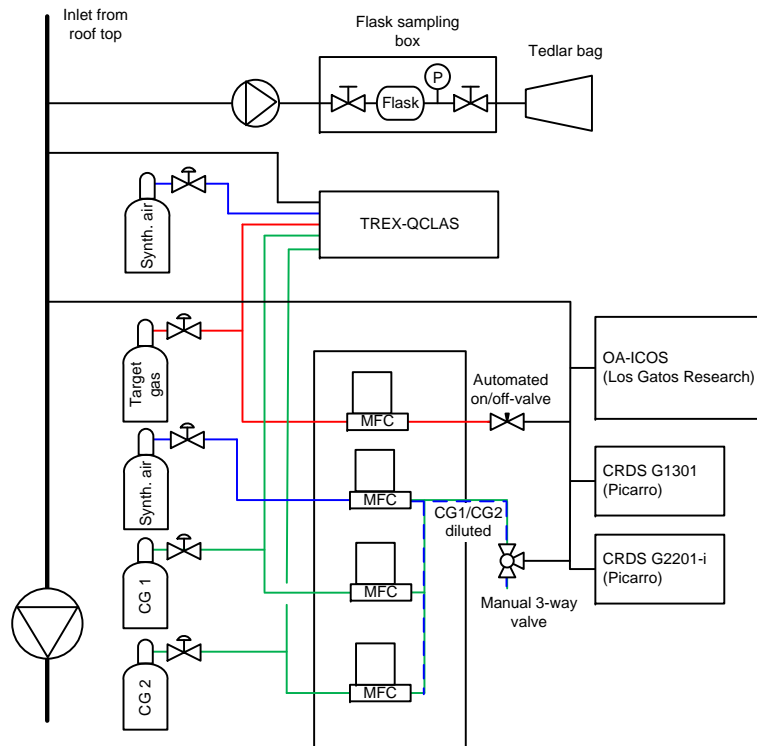


**Figure 3.** Schematics of the sampling setup used in the interlaboratory comparison campaign. Ambient air was continuously sampled from the rooftop of the building, and split from the main line to the batch sampling unit (bags and flasks), to the TREX-QCLAS system and to the continuous flow CRDS and OA-ICOS spectrometers. The laser spectrometers were additionally supplied with the calibration gases CG 1, CG 2 and the target gas to determine calibration factors and repeatability.

## Real-time analysis of $\delta^{13}\text{C}$ - and $\delta\text{D-CH}_4$ in ambient air with laser spectroscopy

S. Eyer et al.

Title Page	
Abstract	Introduction
Conclusions	References
Tables	Figures
◀	▶
◀	▶
Back	Close
Full Screen / Esc	
Printer-friendly Version	
Interactive Discussion	





**Real-time analysis of  $\delta^{13}\text{C}$ - and  $\delta\text{D}$ - $\text{CH}_4$  in ambient air with laser spectroscopy**

S. Eyer et al.

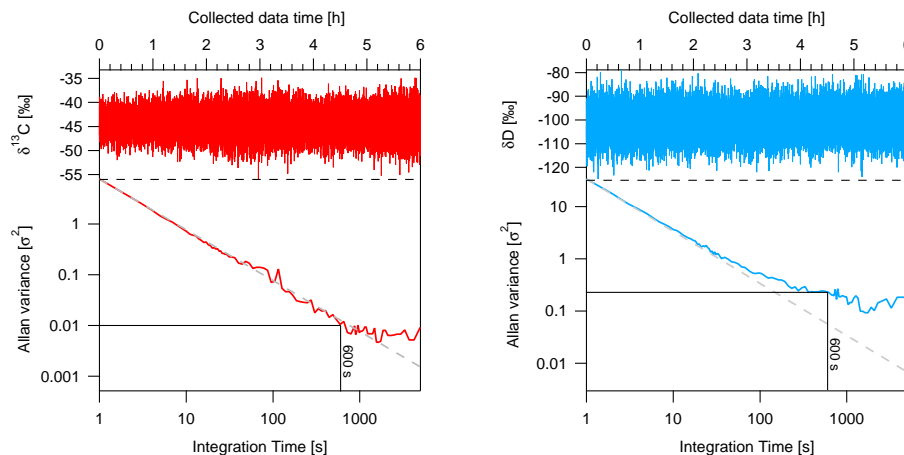


**Figure 5.** Allan variance plots for  $\delta^{13}\text{C}\text{-CH}_4$  (left) and for  $\delta\text{D}\text{-CH}_4$  (right) using 750 ppm  $\text{CH}_4$ . The upper plot shows the corresponding time series of  $\delta$ -values recorded at one second temporal resolution. At 600 s spectral averaging, the square root of the Allan variance indicates a precision of 0.1 ‰ for  $\delta^{13}\text{C}\text{-CH}_4$  and 0.5 ‰ for  $\delta\text{D}\text{-CH}_4$ .

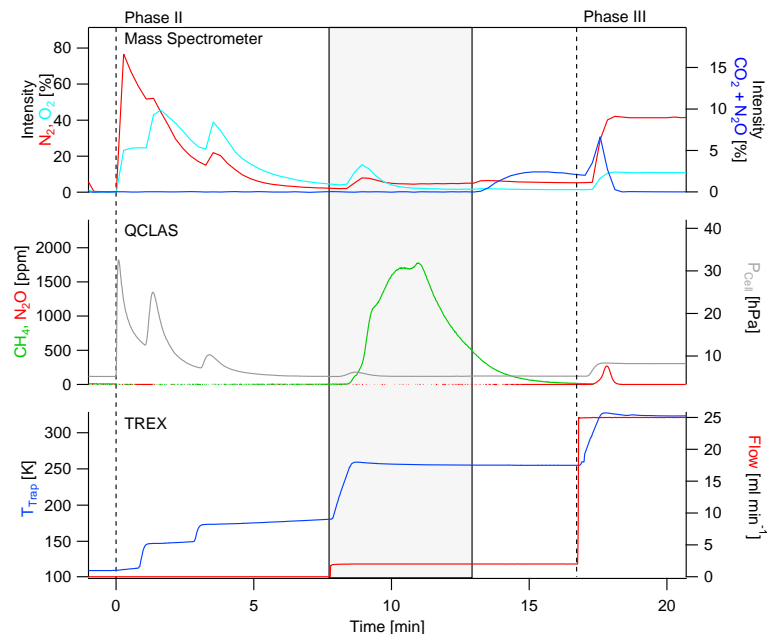


**Figure 6.** Phase II (desorption) and phase III (conditioning) of the  $\text{CH}_4$  preconcentration cycle by TREX. Mass spectrometer results (upper graph) indicate that the bulk gases  $\text{N}_2$  and  $\text{O}_2$  leave the trap shortly after decoupling the trap from the cold-plate and heating successively to 145 K (1 min) and 175 K (3 min), but a small reminder is also released in the main  $\text{CH}_4$  desorption step (see text for details). QCLAS measurements (middle graph) display that  $\text{CH}_4$  desorption is initiated by heating the trap to 258 K (8 min) and purging it with  $2 \text{ mL min}^{-1}$  synthetic air in forward flow direction; the gray shaded area indicates the period, during which the desorbed methane is filled into the gas cell of the laser spectrometer. In phase III (conditioning) the trap is heated up to 323 K and purged with  $25 \text{ mL min}^{-1}$  of high-purity synthetic air. The bottom graph exhibits the trap temperatures and flows of synthetic air in the preconcentration device (TREX).

Title Page

Abstract

Introduction

Conclusions

References

Tables

Figures

◀

▶

◀

▶

Back

Close

Full Screen / Esc

Printer-friendly Version

Interactive Discussion



## Real-time analysis of $\delta^{13}\text{C}$ - and $\delta\text{D-CH}_4$ in ambient air with laser spectroscopy

S. Eyer et al.

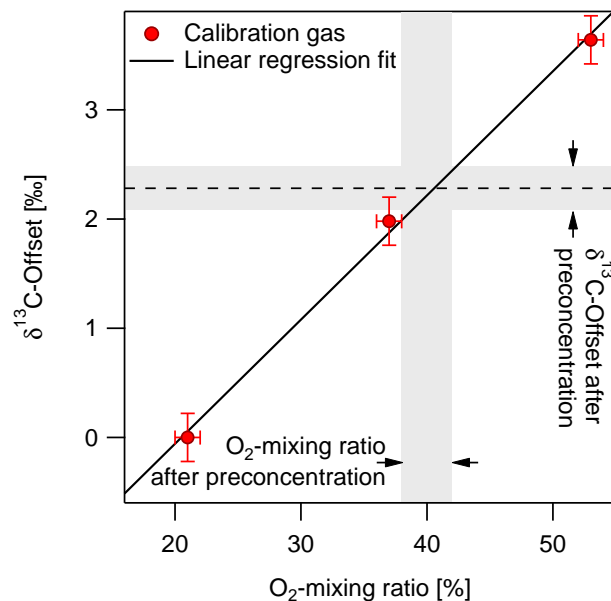


**Figure 7.**  $\delta^{13}\text{C}$ -offset as a function of  $\text{O}_2$  mole fraction determined from measurements of calibration gases without preconcentration with the QCLAS. This effect was found to be constant for  $\text{CH}_4$ -mole fractions from 600 to 1000 ppm. The grayed region shows the ranges of the  $\text{O}_2$ -mole fractions in the QCLAS-cell after preconcentration and the resulting offset in the  $\delta^{13}\text{C}$  values for typical TREX operation as determined from a series of experiments. The dashed horizontal line represents the offset in  $\delta^{13}\text{C}$  values of 2.3‰ used as a correction throughout the measurement campaign.

Title Page

Abstract

Introduction

Conclusions

References

Tables

Figures

◀

▶

◀

▶

Back

Close

Full Screen / Esc

Printer-friendly Version

Interactive Discussion



**Real-time analysis of  $\delta^{13}\text{C}$ - and  $\delta\text{D}$ - $\text{CH}_4$  in ambient air with laser spectroscopy**

S. Eyer et al.

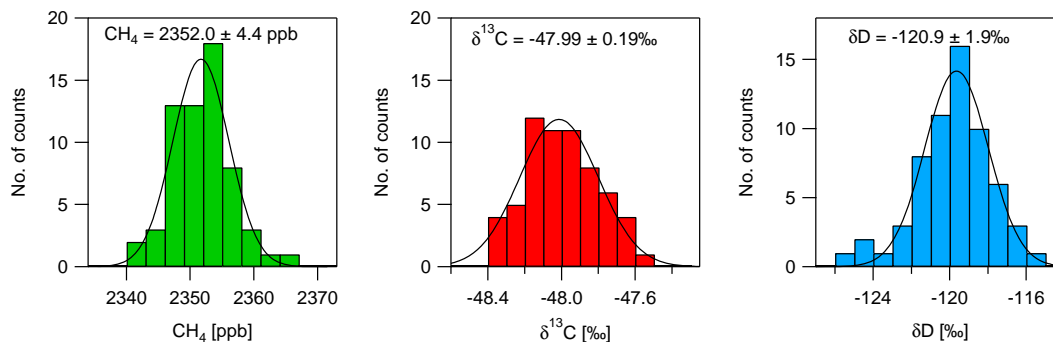


**Figure 8.** Repeated measurements of pressurized air (target gas) by TREX-QCLAS over two weeks throughout the interlaboratory comparison campaign.  $\text{CH}_4$  mole fractions and relative differences of isotope ratios ( $\delta^{13}\text{C}$ ,  $\delta\text{D}$ ) were plotted as a histogram with bin widths of 3 ppb ( $\text{CH}_4$ ), 0.1‰ ( $\delta^{13}\text{C}$ ) and 1‰ ( $\delta\text{D}$ ), respectively. The uncertainty is given as the  $1\sigma$  standard deviation.

[Title Page](#)[Abstract](#)[Introduction](#)[Conclusions](#)[References](#)[Tables](#)[Figures](#)[◀](#)[▶](#)[◀](#)[▶](#)[Back](#)[Close](#)[Full Screen / Esc](#)[Printer-friendly Version](#)[Interactive Discussion](#)

## Real-time analysis of $\delta^{13}\text{C}$ - and $\delta\text{D}$ - $\text{CH}_4$ in ambient air with laser spectroscopy

S. Eyer et al.

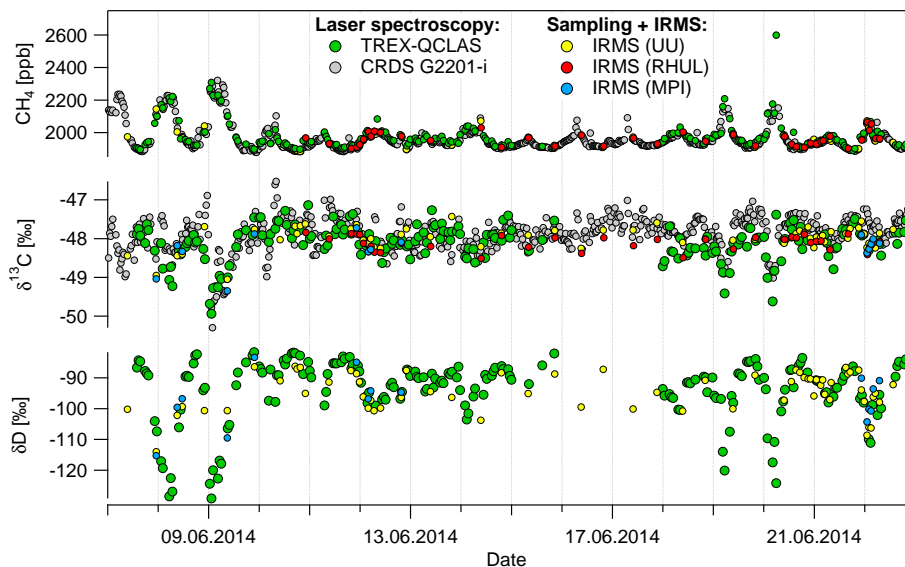


**Figure 9.**  $\text{CH}_4$  mole fractions and isotopic composition analyzed during the interlaboratory comparison campaign in real-time by the laser spectroscopic techniques: TREX-QCLAS ( $\text{CH}_4$ ,  $\delta^{13}\text{C}$ ,  $\delta\text{D}$ ), CRDS G2201-i ( $\text{CH}_4$ ,  $\delta^{13}\text{C}$ ), and on glass flask/bag samples with IRMS by UU ( $\text{CH}_4$ ,  $\delta^{13}\text{C}$ ,  $\delta\text{D}$ ), MPI ( $\text{CH}_4$ ,  $\delta^{13}\text{C}$ ,  $\delta\text{D}$ ) and RHUL ( $\text{CH}_4$ ,  $\delta^{13}\text{C}$ ).

Title Page

Abstract

Introduction

Conclusions

References

Tables

Figures



Back

Close

Full Screen / Esc

Printer-friendly Version

Interactive Discussion



Real-time analysis of  $\delta^{13}\text{C}$ - and  $\delta\text{D-CH}_4$  in ambient air with laser spectroscopy

S. Eyer et al.

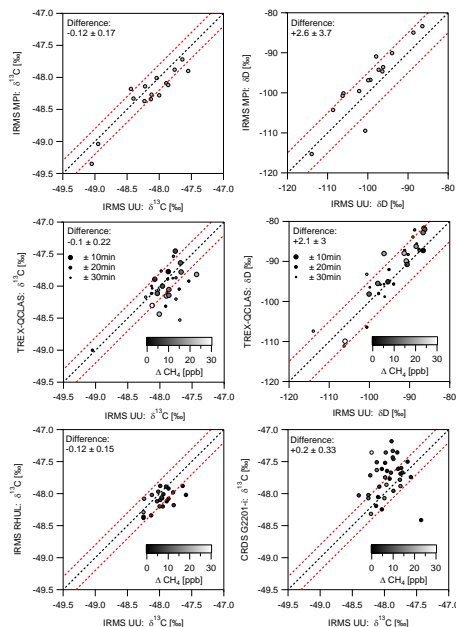


**Figure 10.** Correlation diagrams for  $\text{CH}_4$  isotope ( $\delta^{13}\text{C}$ ,  $\delta\text{D-CH}_4$ ) measurements in ambient air by different techniques and laboratories. The dashed black line is the 1 : 1 line, the red dashed lines indicate the WMO compatibility goals of  $\pm 0.2\text{‰}$  for  $\delta^{13}\text{C}$  and  $\pm 5\text{‰}$  for  $\delta\text{D}$ . Results of individual techniques are corrected to a common scale based on MPI results for a pressurized air target gas. For the middle and bottom graphs differences in  $\text{CH}_4$  mole fractions in gas samples are represented by the shading (black: identical mole fractions, white: 30 ppb difference). Top: IRMS analysis on glass flasks by the Stable Isotope Laboratory of MPI vs. UU for  $\delta^{13}\text{C-CH}_4$  (left) and  $\delta\text{D-CH}_4$  (right); Middle: TREX-QCLAS analysis by Empa vs. IRMS analysis on glass flasks by UU for  $\delta^{13}\text{C-CH}_4$  (left) and  $\delta\text{D-CH}_4$  (right). The temporal difference between TREX-QCLAS analysis and glass flask sampling is indicated by the point size (big:  $\pm 10$  min, medium:  $\pm 20$  min, small:  $\pm 30$  min); Bottom: IRMS analysis on bag samples by RHUL (left) and CRDS analysis by Eawag (right) vs. IRMS analysis on glass flasks by UU for  $\delta^{13}\text{C-CH}_4$ .

Title Page

Abstract

Introduction

Conclusions

References

Tables

Figures



Back

Close

Full Screen / Esc

Printer-friendly Version

Interactive Discussion





